Received: 31 July 2020 | Accepted: 28 September 2020

DOI: 10.1113/EP088977

Experimental Physiology WILEY

RESEARCH PAPER

Breath holding as an example of extreme hypoventilation: experimental testing of a new model describing alveolar gas pathways

Anna Taboni[1] | Nazzareno Fagoni[2] | Timothée Fontolliet[1,3] | Gabriele Simone Grasso[4] | Christian Moia[1,3] | Giovanni Vinetti[2] | Guido Ferretti[1,2,3]

[1] Department of Anaesthesiology, Pharmacology, Intensive Care and Emergencies, University of Geneva, Geneva, Switzerland

[2] Department of Molecular and Translational Medicine, University of Brescia, Brescia, Italy

[3] Department of Basic Neurosciences, University of Geneva, Geneva, Switzerland

[4] School of Medicine and Surgery, University of Milano – Bicocca, Monza, Italy

Correspondence
Anna Taboni, Department of Anaesthesiology, Pharmacology, Intensive Care and Emergencies, University of Geneva, 1 rue Michel Servet, 1211 Geneva 4, Switzerland.
Email: anna.taboni@unige.ch

Funding information
This study was supported by Swiss National Science Foundation, Berne, Switzerland (grant number 32003B_179448; to G.F.).

Edited by: Andrew Sheel

Abstract

According to the hypothesis that alveolar partial pressures of O_2 and CO_2 during breath holding (BH) should vary following a hypoventilation loop, we modelled the alveolar gas pathways during BH on the O_2–CO_2 diagram and tested it experimentally during ambient air and pure oxygen breathing. In air, the model was constructed using the inspired and alveolar partial pressures of O_2 (P_{IO_2} and P_{AO_2}, respectively) and CO_2 (P_{ICO_2} and P_{ACO_2}, respectively) and the steady-state values of the pre-BH respiratory exchange ratio (RER). In pure oxygen, the model respected the constraint of $P_{ACO_2} = -P_{AO_2} + P_{IO_2}$. To test this, 12 subjects performed several BHs of increasing duration and one maximal BH at rest and during exercise (30 W cycling supine), while breathing air or pure oxygen. We measured gas flows, P_{AO_2} and P_{ACO_2} before and at the end of all BHs. Measured data were fitted through the model. In air, $P_{IO_2} = 150 \pm 1$ mmHg and $P_{ICO_2} = 0.3 \pm 0.0$ mmHg, both at rest and at 30 W. Before BH, steady-state RER was 0.83 ± 0.16 at rest and 0.77 ± 0.14 at 30 W; $P_{AO_2} = 107 \pm 7$ mmHg at rest and 102 ± 8 mmHg at 30 W; and $P_{ACO_2} = 36 \pm 4$ mmHg at rest and 38 ± 3 mmHg at 30 W. By model fitting, we computed the RER during the early phase of BH: 0.10 [95% confidence interval (95% CI) = 0.08–0.12] at rest and 0.13 (95% CI = 0.11–0.15) at 30 W. In oxygen, model fitting provided P_{IO_2}: 692 (95% CI = 688–696) mmHg at rest and 693 (95% CI = 689–698) mmHg at 30 W. The experimental data are compatible with the proposed model, within its physiological range.

KEYWORDS
alveolar gas, apnoea, breath holding, carbon dioxide, oxygen, O_2–CO_2 diagram

1 | INTRODUCTION

The alveolar gas composition has been ascribed among the factors limiting maximal breath hold (BH) duration and depth (Fitz-Clarke, 2018). In fact, a combination of hypoxia and hypercapnia leads to the volitional or conventional breaking point of BH and defines the limits of safety during prolonged BH (Lindholm & Lundgren, 2009). These limits have been settled at the boundaries of the anoxic collapse and

of the hypercapnic narcosis regions on an O_2–CO_2 diagram (Ferretti, 2001; Ferretti et al., 1991; Rahn & Fenn, 1955). Thus, the construction of a physiological model, allowing *a priori* predictions of alveolar gas composition at the end of maximal BH, would be of practical importance in diving and extreme hypoventilation and should account for the alveolar pathways during BH, which have been studied for a long time (Agostoni, 1963; Fagoni et al., 2017; Ferretti, 2001; Ferretti et al., 1991; Lanphier & Rahn, 1963; Lin, Lally, Moore, & Hong, 1974, 1983; Lindholm & Lundgren, 2006; Otis, Rahn, & Fenn, 1948; Taboni, Fagoni, Moia, Vinetti, & Ferretti, 2019). To the best of our knowledge, only fragmented mathematical models have been proposed so far, and separately for the time course of alveolar partial pressures of O_2 and CO_2 (P_{AO_2} and P_{ACO_2}, respectively; Hong et al., 1971; Hyde, Puy, Raub, & Forster, 1968; Lanphier & Rahn, 1963; Lin, 1988). The former was considered linear in the first minutes of BH, but slowing down over longer times; the latter was treated as a capacitor charge-like exponential. These analyses are strictly empirical and descriptive, and the theoretical physiological context into which they can be interpreted conveniently has been poorly defined so far.

Owing to the different solubility in blood and cells between CO_2 and O_2, the amount of CO_2 that is loaded into rapidly exchanging tissues at the beginning of a hypoventilation is larger than the amount of O_2 that is removed from the same tissues, before the new equilibrium is attained. This has led to the creation of the concept of a hypoventilation loop (Farhi & Rahn, 1955; Rahn & Fenn, 1955). When hypoventilation begins, the alveolar gas composition on the O_2–CO_2 diagram draws a concave upward curve before attaining a new steady-state value on the prevailing respiratory exchange ratio (RER) line in the preceding steady-state condition (Figure 1). Theoretically, this is the case for all degrees of hypoventilation, although experimental validation is hard to obtain in awake healthy subjects, especially because it is difficult to maintain sustained hypoventilation for the requested time in controlled breathing conditions. The most complete experiment validating the hypoventilation loop concept is still that by Rahn and Otis (1949), who used an artificial increase of dead space to induce acute alveolar hypoventilation. In that study, the authors analysed the alveolar gas composition every minute for 10 min after inducing acute hypoventilation and found that the alveolar pathway initially moved leftward and then upward on the O_2–CO_2 diagram (Rahn & Otis, 1949: their figure 5). Subsequently, Farhi & Rahn (1955) proposed that the alveolar pathway of unsteady states moves on exponential functions.

In this context, BH can be considered the most extreme example of hypoventilation. In fact, when BH begins, the sudden fall of ventilation generates an unsteady-state condition, in which the alveolar pathway on an O_2–CO_2 diagram might follow those predicted by Rahn and Fenn (1955) for the hypoventilation loop corresponding to a negligible alveolar ventilation (extreme hypoventilation loop). If this hypothesis is correct, the alveolar gas composition at the end of BH of increasing duration should provide P_{AO_2} and P_{ACO_2} values lying on a segment of the extreme hypoventilation loop. This segment should lie between the alveolar gas composition at the start of BH and at the interception with the volitional breaking point curve of BH (Lin et al., 1974).

New Findings

- **What is the central question of this study?**
  We modelled the alveolar pathway during breath holding on the hypothesis that it follows a hypoventilation loop on the O_2–CO_2 diagram.
- **What is the main finding and its importance?**
  Validation of the model was possible within the range of alveolar gas compositions compatible with consciousness. Within this range, the experimental data were compatible with the proposed model. The model and its characteristics might allow predictions of alveolar gas composition whenever the alveolar ventilation goes to zero; for example, static and dynamic breath holding at the surface or during ventilation/intubation failure in anaesthesia.

The aim of the present study was to test the hypothesis that the alveolar pathway during BH follows the pattern described by the extreme hypoventilation loop. To this end: (i) we modelled the extreme hypoventilation loop mathematically; (ii) we measured the alveolar gas composition at the end of a series of BHs over a wide range of durations (from 0 s to maximal) and experimental conditions (rest, light exercise, air breathing and pure oxygen breathing); and (iii) we fitted experimental data to the model, at least for those parts of it that lie in the area compatible with consciousness on the O_2–CO_2 diagram.

2 | METHODS

2.1 | Ethical approval

All subjects gave their written informed consent after having received a detailed description of the methods and experimental procedures of the study. This study conformed to the standards set by the *Declaration of Helsinki*, except for registration in a database. Approval was granted by the Commission Cantonale d'Éthique de la Recherche, Canton de Genève, Switzerland (11 July 2018; no. 2018-00913).

2.2 | Subjects

Twelve healthy subjects were enlisted (ten men and two women). Age, body mass and height were 40 ± 8 years, 177 ± 6 cm and 76 ± 9 kg, respectively. Their total lung capacity was 6.68 ± 1.49 l and their residual volume 1.71 ± 0.84 l. Nine subjects were well-trained divers who came from different clubs of northern Italy, one was a top-level

diver from a European national team and two were non-divers who were able to perform a dry resting BH of ≥3 min.

2.3 | Experimental procedure

Experiments were carried out at sea level, in Lignano Sabbiadoro, Italy, in a room at 23 ± 1°C, with relative humidity at 44 ± 7% and with a barometric pressure (P_B) of 764 ± 3 mmHg. The subjects came to the laboratory on two occasions: one for the tests in air, the other for the tests in oxygen.

Upon arrival in the laboratory, the subjects lay supine on a table and, after instrumentation, they were familiarized with the procedures. Pre-BH values were recorded during the last half of 10 min of quiet rest. Then, the subjects performed a series of operator-interrupted BHs of predetermined durations and one maximal volitionally interrupted BH. The scheduled durations were 0, 30, 60, 90, 120, 150 and 180 s for BHs in air and 0, 60, 120, 180, 240, 300 and 360 s for BHs in oxygen. At the end of the procedure at rest, the subject had a short recovery, during which a cycle ergometer (Ergoselect 400; Ergoline GmbH, Bitz, Germany) was mounted on the table. Then, the subject started to pedal at 30 W at 60 r.p.m. in the supine position and continued to exercise until the end of the procedure. Pre-BH values were recorded during 5 min after attainment of steady-state exercise (Ferretti, Fagoni, Taboni, Bruseghini, & Vinetti, 2017). Then, the subjects were asked to perform a series of operator-interrupted BHs (0, 30, 45, 60, 75, 90 and 105 s in air; 0, 60, 90, 120 and 180 s in oxygen) and one maximal, volitionally interrupted BH.

Breath-hold durations were administered in random order among the subjects to avoid possible warm-up effects. Successive BHs were separated by 150 s for recovery and alveolar gas re-equilibration.

On the day of the test in oxygen, experiments were carried out while breathing pure oxygen delivered by means of a two-way non-rebreathing T-shaped valve (Hans Rudolph, Inc., Shawnee, KS, USA). The inhalation port was connected to a 200 l Douglas bag, which was used as a pressure buffer and was filled with 100% O_2 from a high-pressure tank. The O_2 delivery system was connected to the subject at the end of the flowmeter, during instrumentation. After connection, 10 min of quiet breathing was allowed, until attainment of alveolar gas equilibration (Darling, Cournand, Mansfield, & Richards, 1940), before performing the procedure. The O_2 delivery system was kept connected to the subject throughout the entire procedure.

In all conditions and before each BH, subjects were instructed to prepare themselves for a maximal BH, regardless of the scheduled duration. The pre-dive routine of 10 subjects out of 12 consisted of some deep respiratory acts, ending with a maximal inspiration. The remaining two subjects systematically performed lung packing (packed volume of 0.44 ± 0.23 and of 0.36 ± 0.15 l), such that the lung volume at which the BH started in the former was close to and in the latter higher than the subject's total lung capacity. The consistency of the lung volume at the beginning of each BH guaranteed a similar haemodynamic response to BHs within each subject (Mijacika et al., 2017). All BHs were performed with the glottis closed. At the end of each BH, the subject performed a maximal expiration, to allow for expiratory gas analysis.

2.4 | Measurements

Breath-by-breath inspiratory and expiratory flows were measured with an ultrasonic flowmeter (Spiroson; ECO MEDICS AG, Duernten, Switzerland) calibrated with a 3 l syringe. The air fraction of oxygen and carbon dioxide was obtained continuously at the mouth by means of a paramagnetic oxygen analyser (O2100C module; BIOPAC Systems Inc., Goleta, CA, USA) and an infrared CO_2 analyser (CO2100C module; BIOPAC Systems Inc.), respectively, calibrated with two gas mixtures of known composition. The corresponding partial pressures were obtained by multiplying these fractions by the ongoing P_B. Beat-by-beat peripheral haemoglobin oxygen saturation (S_{pO_2}) was monitored at an earlobe by red and infrared light absorption analysis (Nellcor N-595; Nellcor Puritan Bennet Inc., Pleasanton, CA, USA).

All signals were collected and sampled at 200 Hz (MP150 system with AcqKnowledge acquisition and analysis software; BIOPAC Systems Inc.) and stored on a personal computer for subsequent analysis. Respiratory gas fractions and flow traces were aligned for the time delay between the flowmeter and the gas analysers. Flat flowmeter signals provided the beginning, end and duration of BH.

2.5 | Mathematical modelling

Before a BH, the alveolar gas composition at steady state corresponds to that of quiet breathing (Figure 1, point B) lying on the isopleth for steady-state RER (Figure 1, line α). When a BH begins, the alveolar gas composition should follow a pathway of an extreme hypoventilation loop (Figure 1, continuous curve), which is a particular hypoventilation loop, starting from point B of Figure 1 and heading towards a new (virtual) steady state, in which all the alveolar O_2 is replaced by CO_2 (Ferretti, 2001), i.e. the *y*-axis intercept of the steady-state RER isopleth (Figure 1, point C). Mathematically, hypoventilation loops can be described by an exponential equation (Farhi & Rahn, 1955; Rahn & Fenn, 1955), the general form of which is:

$$P_{AO_2} = b \times e^{a \times P_{ACO_2}} + c \quad (1)$$

where *a*, *b* and *c* are the determinants of the exponential equation and have been developed in the Appendix. The curve described by Equation 1 is characterized by the following parameters: (i) P_B; (ii) the inspired partial pressures of O_2 and of CO_2 (P_{IO_2} and P_{ICO_2}; Figure 1, point A); (iii) the RER during pre-BH steady state (Figure 1, line α); (iv) the steady-state pre-BH P_{ACO_2}; and (v) the RER during the early phase of BH (Figure 1, line β), i.e. the RER during BH before the upward bending of the hypoventilation curve takes place (Figure 1, continuous curve). The determinants *a*, *b* and *c* can be expressed as a function of these parameters (see Appendix). When applying Equation 1 to the present experimental data, P_{IO_2}, P_{ICO_2}, the RER during pre-BH

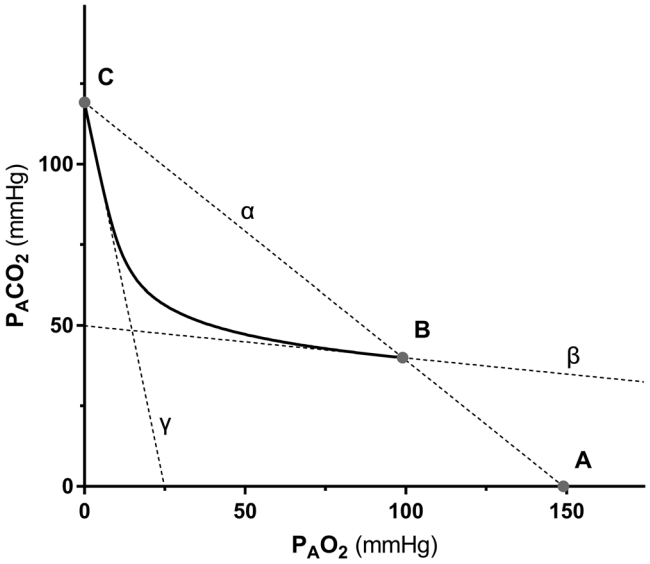

FIGURE 1 Graphical representation of the proposed model for the alveolar pathway during breath holding (continuous curve) in air. This curve, to be followed from point B to point C, represents the alveolar pathway during breath holding. Dashed lines α, β and γ represent the constructing lines. Abbreviations: A, inspired gas composition; B, alveolar gas composition before breath holding; C, *y*-intercept of line α; α, isopleth for the respiratory exchange ratio before breath holding; β, isopleth for the respiratory exchange ratio during the initial part of breath holding; and γ, isopleth for the respiratory exchange ratio = ∞

steady state and the steady-state pre-BH P_{ACO_2}, which were already known, have been inserted manually in the equation, whereas the RER during the early phase of BH was obtained by fitting Equation 1 to the experimental data.

Equation 1 applies for BHs performed in air, in which case nitrogen compensates for pressure changes attributable to differences between the O_2 flux ($\dot{V}_{O_2}$) from the alveoli to the blood and the CO_2 flux ($\dot{V}_{CO_2}$) from the blood to the alveoli. This is not the case when breathing pure oxygen. In fact, whatever the inspired gas composition, at the opening of the glottis the sum of all alveolar gases must be equal to P_B − 47 mmHg. If only two gases are present, as in the case of pure oxygen breathing, the only alveolar gases are O_2 and CO_2, such that $P_{ACO_2} + P_{AO_2} = P_B - 47$ mmHg. At the same time, when the inspired fraction of O_2 (F_{IO_2}) is equal to one, the inspired gas composition is $P_{IO_2} = P_B - 47$ mmHg. Consequently, all possible values of P_{AO_2} and P_{ACO_2} while breathing pure oxygen, when plotted on an O_2–CO_2 diagram, are bound to lie along a straight line with a slope of minus one and intercepting the *x*-axis at a point corresponding to the composition of the inspired air. Such a line can be described as follows:

$$P_{ACO_2} = -P_{AO_2} + P_{IO_2} \quad (2)$$

Thus, in pure oxygen, the alveolar pathway during BH can follow only the straight line described by Equation 2 (see Appendix for details).

2.6 | Data treatment

The P_{AO_2} and P_{ACO_2} were obtained from the alveolar plateau recorded during the maximal expiration at the end of each BH. During the pre-BH steady state, when no alveolar plateau was recognized, the end-tidal partial pressures of O_2 and CO_2 where retained as a measure of P_{AO_2} and P_{ACO_2}, respectively. Pre-BH steady-state P_{AO_2} and P_{ACO_2} were computed on the last 20 breaths, 30 s before the first apnoea in each set of conditions. Pre-BH steady-state RER (ssRER) was computed by means of Equation 3 (Rahn & Fenn, 1955) with data obtained in air. Equation 3 is based on the pre-BH steady-state partial pressures of gas:

$$\text{ssRER} = \frac{P_{ACO_2} \times (1 - F_{IO_2})}{P_{IO_2} - P_{AO_2} - P_{ACO_2} \times F_{IO_2}} \quad (3)$$

2.7 | Statistical analysis

Data are presented as the mean ± SD. Differences between experimental conditions, *i.e.* in air and in oxygen, and at rest and during exercise, were investigated with a two-way ANOVA. Tukey's *post hoc* test was used to isolate differences. Least-squares fitting of Equations 1 and 2 was performed using non-averaged data points of the whole group of subjects obtained in air and in pure oxygen, respectively. Equation 1 fitting was performed by constraining P_{IO_2}, P_{ICO_2}, pre-BH ssRER and pre-BH steady-state alveolar gas composition with experimental data and provided the RER during the early phase of BH (see Appendix for details), which is presented as the mean and 95% confidence interval. Equation 2 was fitted by allowing P_{IO_2} to vary freely. Differences were considered significant when $P < 0.05$. The statistical software Prism (v.7; GraphPad Software LLC, San Diego, CA, USA) was used.

3 | RESULTS

After the end of a maximal BH, the end-tidal fraction of O_2 and CO_2 normalized within 150 s in all conditions (14 ± 7 breaths, corresponding to 49 ± 27 s).

In air, ssRER was 0.83 ± 0.16 at rest and 0.77 ± 0.14 during exercise ($P = 0.3276$). Pre-BH steady-state P_{AO_2} and P_{ACO_2} are reported in Table 1. The composition of the alveolar gas at the end of 0 s and maximal BH is also shown in Table 1.

Maximal BH durations in air were 221 ± 54 s at rest and 88 ± 33 s during exercise ($P < 0.0001$ *versus* rest); in oxygen, maximal BH duration was 404 ± 110 s at rest ($P < 0.0001$ *versus* air) and 141 ± 40 s during exercise ($P < 0.0001$ *versus* rest in oxygen, $P = 0.2316$ *versus* in air). At the end of maximal BHs, the expired volumes in air were 3.52 ± 0.66 l at rest and 3.13 ± 0.80 l during exercise ($P = 0.6433$ *versus* rest), and in oxygen they were 2.53 ± 1.12 l at rest ($P = 0.0329$ *versus* air) and 2.54 ± 0.63 l during exercise ($P > 0.9999$ *versus* rest in oxygen). In air, the minimum S_{pO_2} did not vary significantly between rest and

TABLE 1 Alveolar gas composition during the steady state before breath holding and at the end of 0 s and of maximal breath holds in all four conditions

		In ambient air		In pure oxygen	
Time	Alveolar gas	At rest	During exercise	At rest	During exercise
Pre-breath hold steady state	P_{AO_2}	107 ± 7	102 ± 8	647 ± 19*	655 ± 24*
	P_{ACO_2}	36 ± 4	38 ± 3	40 ± 16	39 ± 7
0 s breath holds	P_{AO_2}	118 ± 10	105 ± 8	655 ± 18*	659 ± 12*
	P_{ACO_2}	35 ± 5	40 ± 2*	33 ± 4	38 ± 3*
Maximal breath holds	P_{AO_2}	46 ± 14†,‡	49 ± 8†,‡	631 ± 18*,†	634 ± 12*,†
	P_{ACO_2}	51 ± 6†,‡	53 ± 5†,‡	53 ± 5†,‡	57 ± 1†,‡

Abbreviations: P_{ACO_2}, alveolar partial pressure of CO_2; and P_{AO_2}, alveolar partial pressure of O_2.
Values are the mean ± SD. Differences among rows and columns were investigated by means of a two-way ANOVA and isolated with Tukey's test.
*$P < 0.05$ *versus* breath holds in air.
†$P < 0.05$ *versus* 0 s breath holds.
‡$P < 0.05$ *versus* steady state before breath holding.

exercise (81 ± 12 % and 82 ± 12%, respectively, $P = 0.7391$) and was reached 23 ± 5 s and 26 ± 4 s after the end of the BH, respectively ($P = 0.0930$). In oxygen, S_{pO_2} was unchanged and equal to 100%. Loss of consciousness did not occur in any subject.

In air, most of the experimental data lay on the horizontal part of the extreme hypoventilation loop, both at rest (Figure 2, upper panel, filled circles) and during exercise (Figure 2, lower panel, filled circles). In these conditions, Equation 1 fitting provided a RER during the early phase of BH equal to 0.10 at rest (95% confidence interval: 0.08–0.12) and 0.13 during exercise (95% confidence interval: 0.11–0.15). In pure oxygen, Equation 2 fitting provided a P_{IO_2} equal to 692 mmHg at rest (95% confidence interval: 688–696 mmHg; Figure 2, upper panel, open circles) and 693 mmHg during exercise (95% confidence interval: 689–698 mmHg; Figure 2, lower panel, open circle). Owing to CO_2 sensor saturation during some of the longer BHs, one BH in air at rest and five BHs at rest and nine BHs during exercise in oxygen where excluded from fitting and subsequent analysis.

4 | DISCUSSION

This study provides the first mathematical model describing the pathway of alveolar gas composition during BHs based on the hypothesis that it might follow an extreme hypoventilation loop (Ferretti, 2001; Rahn & Fenn, 1955), at rest and during exercise, both in air and in oxygen. The loop is curvilinear in air (Equation 1), whereas in BHs performed in pure oxygen it is necessarily constrained to a straight line (Equation 2).

If we analyse the extreme hypoventilation loop of BH performed in ambient air, we can identify two segments: the first, almost horizontal, is characterized by a decrease in P_{AO_2} that is larger than the corresponding increase in P_{ACO_2}, whereas the second, bending upward, is characterized by a smaller decrease in P_{AO_2} than the corresponding increase in P_{ACO_2}. The flat segment reflects CO_2 storage in tissues rather than in the alveoli (Farhi & Rahn, 1960; Fitz-Clarke, 2018) while the O_2 stores are emptied (Farhi & Rahn, 1955), resulting in an extremely low RER. In fact, CO_2 has a much larger solubility coefficient in tissues than O_2 (respectively, 0.515 and 0.0214 ml of gas per millilitre of human plasma at sea level at 37°C; Christmas & Bassingthwaighte, 2017). Thus, *ceteris paribus*, CO_2 storage capacity is some 25 times larger than O_2 storage capacity. Rapidly exchanging tissues are involved for the most part, namely blood and lungs, characterized by relatively small capacity and low (fast) equilibrium time constants (Farhi & Rahn, 1960; Linér & Linnarsson, 1994). The muscle tissue might also be involved, but although the muscles have a larger CO_2 storage capacity (~ 10 l of CO_2), their storage time constant is slower (~ 30 min; Linér & Linnarsson, 1994). Conversely, only a small amount of the alveolar O_2 taken up by the body is replaced by O_2 coming from rapidly exchanging O_2 stores. The very low RER during the early phase of BH provided by fitting Equation 1 was in line with a previous study (Otis et al., 1948), in which the authors calculated an RER ranging from 0.1 to 0.22 at sea level in ambient air at rest. A negative RER in certain BH segments has also been demonstrated (Ferretti et al., 1991), owing to reversal of CO_2 flux at the alveolar–capillary barrier (Lindholm & Linnarsson, 2002).

The upward bending of the extreme hypoventilation loop should then start when the gas store re-equilibration is almost complete and the new equilibrium between gas pressure in tissues and alveoli is almost attained. In these conditions, the O_2 gradient sustaining O_2 uptake tends to zero while the CO_2 produced by metabolism is still added to the alveoli, thus RER tends toward infinity. The $\dot{V}_{O_2}$ in the final part of the curve might be sustained, in part, by changes in blood O_2 stores, through an increase in O_2 delivery associated with the involuntary breathing movements (Palada et al., 2008) and incurring arterial and venous haemoglobin desaturation (Lindholm, Sundblad, & Linnarsson, 1999, 2002), and by changes in muscle O_2 stores, which are known to be enhanced in divers (Elia et al., 2019). Moreover, incoming hypoxia might also determine a switch to anaerobic lactic acid metabolism, leading to depletion of the blood bicarbonate pool and an increase in $\dot{V}_{CO_2}$ during the second part of the curve. However, following this second part of the extreme hypoventilation loop, alveolar gas composition would go beyond that compatible

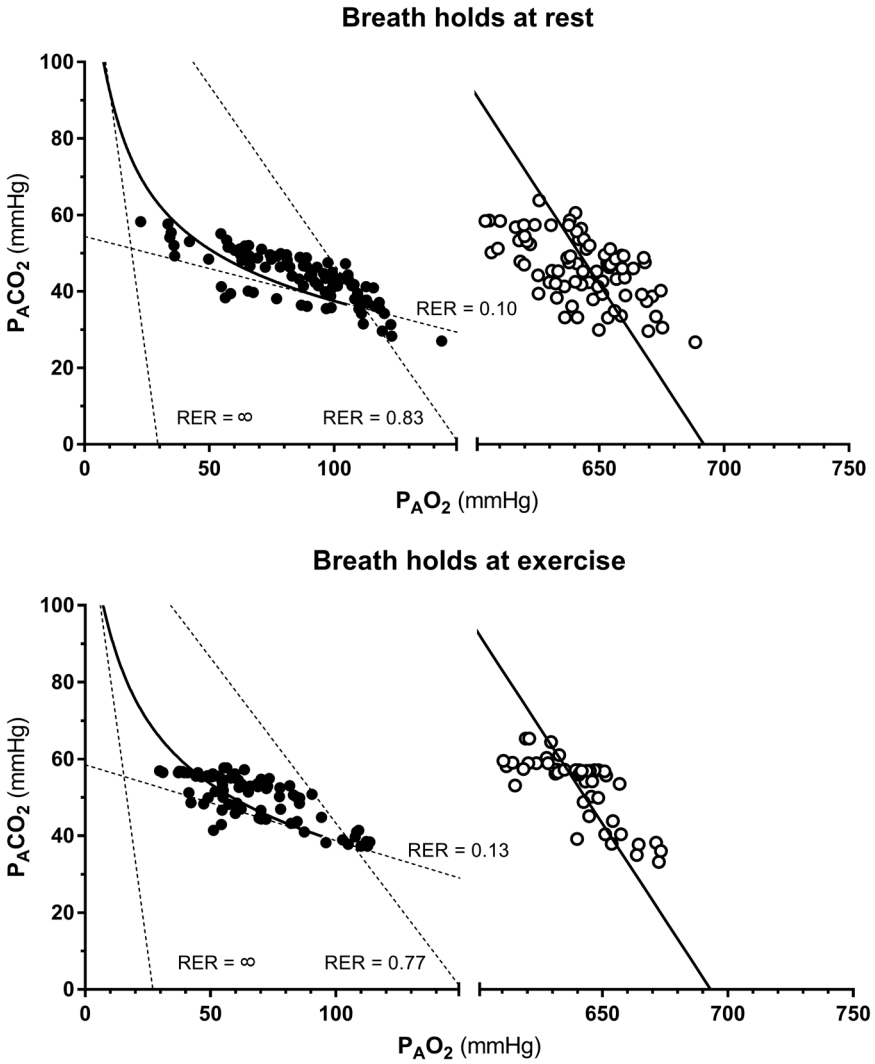

FIGURE 2 Alveolar gas composition at the end of all breath holds at rest (upper panel, 'Breath holds at rest') and during exercise (lower panel, 'Breath holds at exercise'), in air (filled circles) and in oxygen (open circles). Continuous lines represent the fitting functions, which correspond to Equation 1, which is the extreme hypoventilation loop in air ($R^2 = 0.24$ at rest and $R^2 = 0.15$ during exercise) and to Equation 2 in oxygen ($R^2 = 0.65$ at rest and $R^2 = 0.84$ during exercise). Dashed lines represent the constructing straight lines of the extreme hypoventilation loop (see Appendix). Abbreviations: P_{ACO_2} and P_{AO_2}, alveolar partial pressure of carbon dioxide and of oxygen, respectively; and RER, respiratory exchange ratio. Every circle represents a single alveolar gas composition

with life or simply with consciousness. Thus, the steep part of the extreme hypoventilation loop cannot be tested experimentally, and the overall pattern of this curve is condemned to remain a theoretical concept. Notwithstanding, the experimental data are compatible with the model, at least in its flattest part up to its flexus; therefore, the hypothesis that alveolar gas patterns during BHs follow an extreme hypoventilation loop cannot be rejected on the basis of the present results.

When BHs are performed during exercise, the cardiac output during BH is higher than at rest, peripheral O_2 desaturation occurs more rapidly (Lindholm & Linnarsson, 2002; Sivieri et al., 2015), and the decrease of P_{AO_2} and increase of P_{ACO_2} during BH are more rapid (Taboni et al., 2018). Given that the extreme hypoventilation loop reflects alveolar gas compositions rather than time, we can speculate that the differences in the metabolic rate (rest *versus* exercise) or in the amount of O_2 stores (lung volume or haemoglobin mass) will not affect the shape of the alveolar pathway during BH, but only the speed at which it is travelled. Likewise, the lung volume does not affect the alveolar pathway during BHs performed in pure oxygen, which is described by Equation 2. In fact, when BH is performed in pure oxygen, the mismatch between $\dot{V}_{O_2}$ and $\dot{V}_{CO_2}$ results in a decrease in lung volumes (Klocke & Rahn, 1959). Nevertheless, the O_2–CO_2 diagram describes only the partial pressures of O_2 and CO_2, and thus does not account for changes in lung volumes.

When BHs are performed in pure oxygen, our model affirms that the alveolar pathway is constrained by Equation 2. As shown in Figure 2, the fitting of experimental data to Equation 2 provides an *x*-intercept slightly lower than the expected P_{IO_2}, *i.e.* $P_B - 47$ mmHg = 716 mmHg. To explain this discrepancy, we might consider that the oxygen analyser works close to its highest range limit, where a small error in fraction measurement can result in a big difference in pressure. To investigate the alveolar pathways during BH in normobaric pure oxygen, we suggest that the use of a single analyser for all respiratory gases, for example by means of a mass spectrometer, might ease the data analysis.

Previous studies (Hong et al., 1971; Hyde et al., 1968; Lanphier & Rahn, 1963; Lin, 1988) proposed two separate models for the changes of P_{AO_2} and P_{ACO_2} over time. According to those studies, P_{AO_2} decreases linearly with time during the first minutes, and successively decreases at a progressively slower rate. Hong et al. (1971) attributed the slowing down of the P_{AO_2} fall to the progressive decrease in the

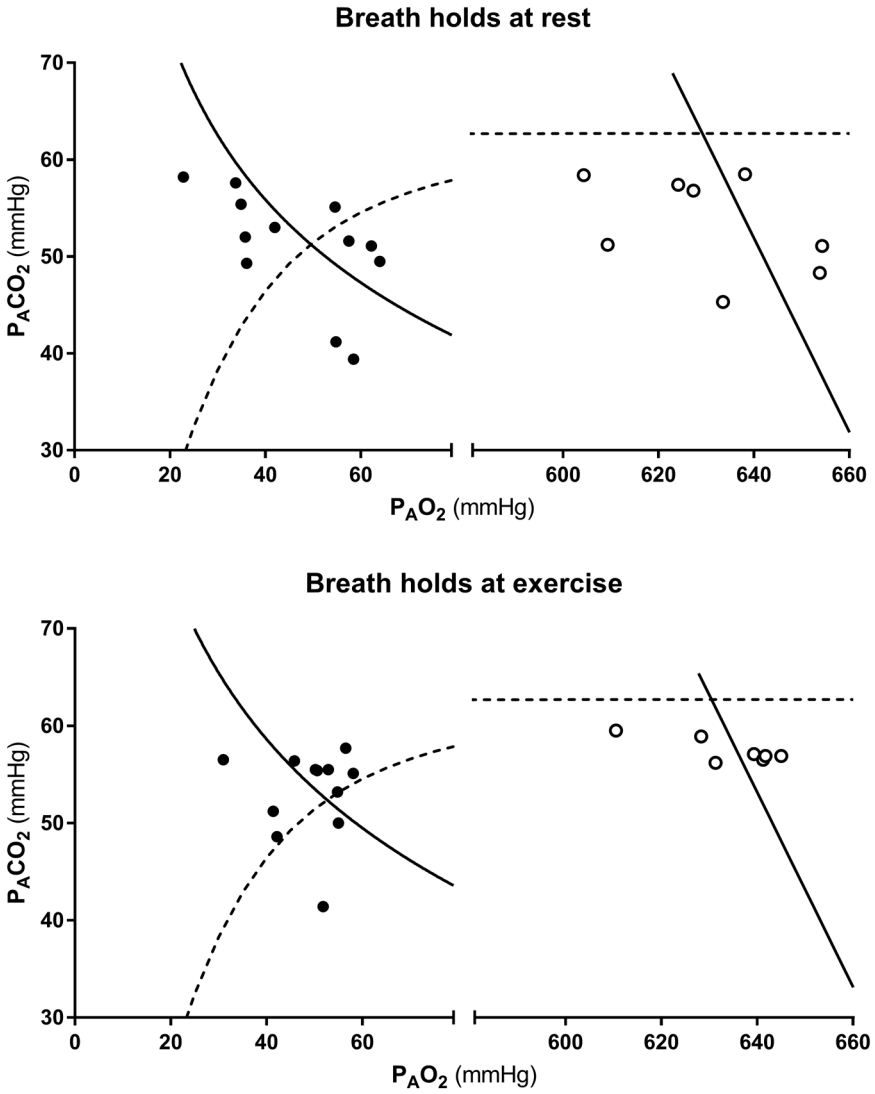

FIGURE 3 Alveolar gas composition at the end of maximal breath holds (filled circles, breath holds in air; open circles, breath holds in oxygen) at rest (upper panel, 'Breath holds at rest') and during exercise (lower panel, 'Breath holds at exercise'). Continuous lines represent the fitting functions, corresponding to Equation 1 in air and Equation 2 in oxygen, as in Figure 2. Dashed lines represent the conventional breaking point curve (Taboni et al., 2019). Abbreviations: P_{ACO_2} and P_{AO_2}, alveolar partial pressure of carbon dioxide and of oxygen, respectively. Every circle represents a single alveolar gas composition

arteriovenous O_2 difference. Concerning the time course of P_{ACO_2}, this was modelled as an exponential function with a plateau. In fact, at the beginning of apnoea, P_{ACO_2} increases rapidly owing to low initial values. This is a consequence of the rapid wash-out caused by the last deep inspiration. When P_{ACO_2} approaches capillary blood CO_2 partial pressure, it rises at a slower rate. The rise of P_{ACO_2} eventually stops when lung shrinking increases P_{ACO_2} up to values that can exceed the arterial partial pressure of CO_2 (Lin, 1988). Moreover, the elevation of P_{ACO_2} generates a CO_2 pressure gradient between the alveolar air and lung tissue, sustaining a flow of CO_2 into the parenchyma. If we assume a two-segment linear decrease for P_{AO_2} (Occam's razor) and we put these linear segments in an equation system with the exponential increase for P_{ACO_2}, in which time is cancelled out, we can obtain a relationship between P_{AO_2} and P_{ACO_2} to be plotted on an O_2–CO_2 diagram and through which experimental data could be fitted. This relationship is characterized by a concave downward curve, starting from the alveolar gas composition preceding BH and moving upward and leftward. The time courses of P_{AO_2} and P_{ACO_2} leading to such an equation, however, have been analysed on the basis of the mere empirical appearance of experimental data, and no underlying physiological model was proposed. This concave downward shape of the resulting equation is not compatible with the concept of an extreme hypoventilation loop (Ferretti, 2001; Rahn & Fenn, 1955), which defines the physiological context of this study. In fact, when BH starts, the alveolar gases move leftward with respect to the ssRER line on the O_2–CO_2 diagram, because BH is not a steady-state condition. Nevertheless, we might argue that after a sufficient amount of time of BH, virtually infinite, we should in principle reach a new steady state and return on the same ssRER line, in a similar manner to what happens during hypoventilations (Rahn & Fenn, 1955), when all O_2 will have been replaced by CO_2 (Figure 1, point C).

The alveolar gas composition at the end of maximal BH can be predicted regardless of the duration of BH by intersecting the experimental extreme hypoventilation loop and the conventional breaking point curve, which has also been modelled recently by fitting experimental data (Taboni et al., 2019). This is demonstrated in Figure 3, where the individual alveolar gas compositions assessed at the end of maximal BH appear closely to intersect the junction between

the extreme hypoventilation loop curves and the conventional breaking point curve. With some approximations, possibly related to interindividual variability, these intersections appear to be good predictors of the alveolar gas composition at the end of maximal BH. Moreover, as long as the conventional breaking point curve (Taboni et al., 2019) relies on data obtained from healthy subjects (Agostoni, 1963; Lin et al., 1974; three and five subjects, respectively) and our model relies on data obtained in divers of different training level, the applicability of these results to other populations (for example, in conditions characterized by significative ventilation–perfusion mismatch), is limited.

The consistency between the predicted alveolar gas composition at the end of maximal BHs with experimental data, both at rest and during exercise, demonstrates that most divers finish their BH at a similar alveolar gas composition, compatible with a state of consciousness, regardless of BH time and the energy expenditure during BH. Consequently, we are confident that these models and predictions can be useful in both static and dynamic BHs at the surface and in other conditions characterized by negligible alveolar ventilation, such as during ventilation/intubation failure in critical care. Moreover, the theoretical background wherein the mathematical model for the extreme hypoventilation loop has been developed can also be applied to controlled hypoventilations; for example, not only when the dead space is increased artificially or owing to pathological conditions, but also during mechanical ventilation in anaesthetized subjects. Eventually, this model could also be applied to deep diving, with some limitations. During dives, alveolar gas composition is influenced not only by changes in pressure but also by lung shrinkage and complete pulmonary shunt at extreme depths (Fitz-Clarke, 2007, 2009). The external body compression during diving determines different turnover rates for tissue O_2 and CO_2 stores when compared with surface BH (Linér & Linnarsson, 1994). Moreover, a non-invasive alveolar gas composition at depth can be obtained only in controlled laboratory conditions, such as in simulated BH dives in a hyperbaric chamber, given the lack of non-invasive sensors for alveolar gases in diving (Vinetti, Lopomo, Taboni, Fagoni, & Ferretti, 2020). Nevertheless, promising results might come from the analysis of the arterial partial pressure of respiratory gases during dives in simulated and real conditions (Bosco et al., 2018, 2020; Muth et al., 2003) and the development of a model for the arterial gas composition.

ACKNOWLEDGEMENTS

The authors are grateful to the divers who volunteered their time to this study and to Alessandro Vergendo and Rosarita Gagliardi from Apnea Evolution Deep Inside Project for collaboration in recruitment of subjects and logistic organization.

COMPETING INTERESTS

None declared.

AUTHOR CONTRIBUTIONS

G.F. conceived and designed the study. A.T., N.F., T.F. and G.S.G. performed the experiments. A.T. and C.M. analysed the data. A.T., G.V., G.S.G. and G.F. interpreted the results of the experiments. A.T. prepared figures and drafted the first version of the manuscript. All authors edited and revised the manuscript. All authors approved the final version and agree to be accountable for all aspects of the work in ensuring that questions related to the accuracy or integrity of any part of the work are appropriately investigated and resolved. All persons designated as authors qualify for authorship, and all those who qualify for authorship are listed.

DATA AVAILABILITY STATEMENT

The datasets generated and analysed during the current study are available from the corresponding author on reasonable request.

ORCID

Anna Taboni https://orcid.org/0000-0002-8198-6574

REFERENCES

Agostoni, E. (1963). Diaphragm activity during breath holding: Factors related to its onset. *Journal of Applied Physiology*, *18*, 30–36.

Bosco, G., Paganini, M., Rizzato, A., Martani, L., Garetto, G., Lion, J., … Moon, R. E. (2020). Arterial blood gases in divers at surface after prolonged breath-hold. *European Journal of Applied Physiology*, *120*, 505–512.

Bosco, G., Rizzato, A., Martani, L., Schiavo, S., Talamonti, E., Garetto, G., … Moon, R. E. (2018). Arterial blood gas analysis in breath-hold divers at depth. *Frontiers in Physiology*, *9*, 1558.

Christmas, K. M., & Bassingthwaighte, J. B. (2017). Equations for O_2 and CO_2 solubilities in saline and plasma: Combining temperature and density dependences. *Journal of Applied Physiology*, *122*, 1313–1320.

Darling, R. C., Cournand, A., Mansfield, J. S., & Richards, D. W. (1940). Studies on the intrapulmonary mixture of gases. I. Nitrogen elimination from blood and body tissue during high oxygen breathing. *Journal of Clinical Investigation*, *19*, 591–597.

Elia, A., Wilson, O. J., Lees, M., Parker, P. J., Barlow, M. J., Cocks, M., & O'Hara, J. P. (2019). Skeletal muscle, haematological and splenic volume characteristics of elite breath-hold divers. *European Journal of Applied Physiology*, *119*, 2499–2511.

Fagoni, N., Taboni, A., Vinetti, G., Bottarelli, S., Moia, C., Bringard, A., & Ferretti, G. (2017). Alveolar gas composition during maximal and interrupted apnoeas in ambient air and pure oxygen. *Respiratory Physiology and Neurobiology*, *235*, 45–51.

Farhi, L. E., & Rahn, H. (1955). Gas stores of the body and the unsteady state. *Journal of Applied Physiology*, *7*, 472–484.

Farhi, L. E., & Rahn, H. (1960). Dynamics of changes in carbon dioxide stores. *Anesthesiology*, *21*, 604–614.

Ferretti, G. (2001). Extreme human breath-hold diving. *European Journal of Applied Physiology*, *84*, 254–271.

Ferretti, G., Costa, M., Ferrigno, M., Grassi, B., Marconi, C., Lundgren, C. E. G., & Cerretelli, P. (1991). Alveolar gas composition and exchange during deep breath-hold diving and dry breath holds in elite divers. *Journal of Applied Physiology*, *70*, 794–802.

Ferretti, G., Fagoni, N., Taboni, A., Bruseghini, P., & Vinetti, G. (2017). The physiology of submaximal exercise: The steady state concept. *Respiratory Physiology and Neurobiology*, *246*, 76–85.

Fitz-Clarke, J. R. (2007). Mechanics of airway and alveolar collapse in human breath-hold diving. *Respiratory Physiology & Neurobiology*, *159*, 202–210.

Fitz-Clarke, J. R. (2009). Lung compression effects on gas exchange in human breath-hold diving. *Respiratory Physiology and Neurobiology*, *165*, 221–228.

Fitz-Clarke, J. R. (2018). Breath-hold diving. *Comprehensive Physiology*, *8*, 585–630.

Hong, S. K., Lin, Y. C., Lally, D. A., Yim, B. J. B., Kominami, N., Hong, P. W., & Moore, T. O. (1971). Alveolar gas exchanges and cardiovascular functions during breath holding with air. *Journal of Applied Physiology*, *30*, 540–547.

Hyde, R. W., Puy, R. J., Raub, W. F., & Forster, R. E. (1968). Rate of disappearance of labeled carbon dioxide from the lungs of humans during breath holding: A method for studying the dynamics of pulmonary CO_2 exchange. *The Journal of Clinical Investigation*, *47*, 1535–1552.

Klocke, F. J., & Rahn, H. (1959). Breath holding after breathing of oxygen. *Journal of Applied Physiology*, *14*, 689–693.

Lanphier, E. H., & Rahn, H. (1963). Alveolar gas exchange during breath holding with air. *Journal of Applied Physiology*, *18*, 478–482.

Lin, Y. C. (1988). Applied physiology of diving. *Sports Medicine*, *5*, 41–56.

Lin, Y. C., Lally, D. A., Moore, T. O., & Hong, S. K. (1974). Physiological and conventional breath-hold breaking points. *Journal of Applied Physiology*, *37*, 291–296.

Lin, Y. C., Shida, K. K., & Hong, S. K. (1983). Effects of hypercapnia, hypoxia, and rebreathing on heart rate response during apnea. *Journal of Applied Physiology*, *54*, 166–171.

Lindholm, P., & Linnarsson, D. (2002). Pulmonary gas exchange during apnoea in exercising men. *European Journal of Applied Physiology*, *86*, 487–491.

Lindholm, P., & Lundgren, C. E. G. (2006). Alveolar gas composition before and after maximal breath-holds in competitive divers. *Undersea & Hyperbaric Medicine*, *33*, 463–467.

Lindholm, P., & Lundgren, C. E. G. (2009). The physiology and pathophysiology of human breath-hold diving. *Journal of Applied Physiology*, *106*, 284–292.

Lindholm, P., Nordh, J., & Linnarsson, D. (2002). Role of hypoxemia for the cardiovascular responses to apnea during exercise. *American Journal of Physiology-Regulatory, Integrative and Comparative Physiology*, *283*, R1227–R1235.

Lindholm, P., Sundblad, P., & Linnarsson, D. (1999). Oxygen-conserving effects of apnea in exercising men. *Journal of Applied Physiology*, *87*, 2122–2127.

Linér, M. H., & Linnarsson, D. (1994). Tissue oxygen and carbon dioxide stores and breath-hold diving in humans. *Journal of Applied Physiology*, *77*, 542–547.

Mijacika, T., Kyhl, K., Frestad, D., Otto Barak, F., Drvis, I., Secher, N. H., … Lav Madsen, P. (2017). Effect of pulmonary hyperinflation on central blood volume: An MRI study. *Respiratory Physiology and Neurobiology*, *243*, 92–96.

Muth, C. M., Radermacher, P., Pittner, A., Steinacker, J., Schabana, R., Hamich, S., … Calzia, E. (2003). Arterial blood gases during diving in elite apnea divers. *International Journal of Sports Medicine*, *24*, 104–107.

Otis, A. B., Rahn, H., & Fenn, W. O. (1948). Alveolar gas changes during breath holding. *The American Journal of Physiology*, *152*, 674–686.

Palada, I., Bakovic, D., Valic, Z., Obad, A., Ivancev, V., Eterovic, D., … Dujic, Z. (2008). Restoration of hemodynamics in apnea struggle phase in association with involuntary breathing movements. *Respiratory Physiology and Neurobiology*, *161*, 174–181.

Rahn, H., & Fenn, W. O. (1955). *A graphical analysis of the respiratory gas exchange: The O_2-CO_2 diagram*. Washington, D.C.: American Physiological Society.

Rahn, H., & Otis, A. B. (1949). Continuous analysis of alveolar gas composition during work, hyperpnea, hypercapnia and anoxia. *Journal of Applied Physiology*, *1*, 717–724.

Sivieri, A., Fagoni, N., Bringard, A., Capogrosso, M., Perini, R., & Ferretti, G. (2015). A beat-by-beat analysis of cardiovascular responses to dry resting and exercise apnoeas in elite divers. *European Journal of Applied Physiology*, *115*, 119–128.

Taboni, A., Fagoni, N., Moia, C., Vinetti, G., & Ferretti, G. (2019). Gas exchange and cardiovascular responses during breath-holding in divers. *Respiratory Physiology & Neurobiology*, *267*, 27–34.

Taboni, A., Vinetti, G., Bruseghini, P., Camelio, S., D'Elia, M., Moia, C., … Fagoni, N. (2018). Cardiovascular responses to dry apnoeas at exercise in air and in pure oxygen. *Respiratory Physiology and Neurobiology*, *255*, 17–21.

Vinetti, G., Lopomo, N. F., Taboni, A., Fagoni, N., & Ferretti, G. (2020). The current use of wearable sensors to enhance safety and performance in breath-hold diving: A systematic review. *Diving and Hyperbaric Medicine*, *50*, 54–65.

SUPPORTING INFORMATION

Additional supporting information may be found online in the Supporting Information section at the end of the article.

How to cite this article: Taboni A, Fagoni N, Fontolliet T, et al. Breath holding as an example of extreme hypoventilation: experimental testing of a new model describing alveolar gas pathways. *Experimental Physiology*. 2020;105:2216–2225. https://doi.org/10.1113/EP088977

APPENDIX

On a O_2–CO_2 diagram, the *x*- and *y*-axes represent the alveolar partial pressure of O_2 (P_{AO_2}) and CO_2 (P_{ACO_2}), respectively. In ambient air, the inspired partial pressures of O_2 (P_{IO_2}) and CO_2 (P_{ICO_2}) are equal to the respective inspired fractions (i.e. F_{IO_2} and F_{ICO_2}, respectively) multiplied by the barometric pressure (P_B). This is represented by point A in Figure 1. The respiratory exchange ratio at the steady state (ssRER) is described by a straight line intercepting the *x*-axis at point A (Figure 1, straight line α). The alveolar gas composition (ssP_{AO_2} and ssP_{ACO_2}), represented in Figure 1 by point B, lies on the ssRER line. When a breath hold (BH) begins, the ventilation suddenly falls and the alveolar gas composition on the O_2–CO_2 diagram moves to the left of point B, following a very low RER (apnRER) line (Figure 1, straight line β; Ferretti, 2001; Otis et al., 1948; Rahn & Fenn, 1955). As long as the metabolic respiratory quotient (ssRER) does not change, the final alveolar gas composition should coincide with the *y*-intercept of the straight line α (Figure 1, point C). Consequently, when moving from point B to point C, the alveolar gas composition should leave the straight line β and bend upwards to reach point C, following the RER line $= +\infty$ (Figure 1, straight line γ). This pathway reflects the rate of adjustments of oxygen and CO_2 stores and can be represented as an exponential function (Farhi & Rahn, 1955; Rahn & Fenn, 1955), described by the following equation:

$$P_{AO_2} = b \times e^{a \times P_{ACO_2}} + c \quad \text{(A1)}$$

When applying Equation A1, P_{AO_2} and P_{ACO_2} are the independent and the dependent variable of the equation, respectively. Nevertheless, this is not to be interpreted as a physiologically defined dependence of P_{ACO_2} on P_{AO_2}.

During BH, the pathway described by Equation A1 starts from point B, where it is tangent to straight line β, and progressively approaches straight line γ (Figure 1, continuous curve). The

mathematical construction can be followed on Figure 1. The straight line α is described by:

$$P_{ACO_2} = m_\alpha \times \left(P_{AO_2} - P_{IO_2}\right) + P_{ICO_2} \quad \text{(A2)}$$

Where m_α is the slope of the straight line α, which is equal to:

$$m_\alpha = \frac{F_{ICO_2} \times (\text{ssRER} - 1) - \text{ssRER}}{F_{IO_2} \times (\text{ssRER} - 1) + 1} \quad \text{(A3)}$$

The coordinates of the three points A, B, and C are:

$$\text{A} = \left(P_{IO_2}, P_{ICO_2}\right) \quad \text{(A4)}$$

$$\text{B} = \left(\frac{\text{ss}P_{ACO_2} + P_{IO_2} \times m_\alpha - P_{ICO_2}}{m_\alpha}, \text{ss}P_{ACO_2}\right) \quad \text{(A5)}$$

$$\text{C} = \left(0, P_{ICO_2} - m_\alpha \times P_{ICO_2}\right) \quad \text{(A6)}$$

The straight line β is described by:

$$P_{ACO_2} = m_\beta \times P_{AO_2} + k_\beta \quad \text{(A7)}$$

where the *y*-intercept, k_β, is:

$$k_\beta = \text{ss}P_{ACO_2} - \frac{m_\beta}{m_\alpha} \times \left(\text{ss}P_{ACO_2} - P_{ICO_2} + P_{IO_2} \times m_\alpha\right) \quad \text{(A8)}$$

and the slope, m_β, is:

$$m_\beta = \frac{\text{ss}F_{ACO_2}\,(\text{apnRER} - 1) - \text{apnRER}}{\text{ss}F_{AO_2}\,(\text{apnRER} - 1) + 1} \quad \text{(A9)}$$

Where ssF_{ACO_2} and ssF_{AO_2} are the steady state alveolar fractions of CO_2 and O_2, respectively.

The straight line γ is described by:

$$P_{ACO_2} = m_\gamma \times P_{AO_2} + k_\gamma \quad \text{(A10)}$$

where the y-intercept k_γ is:

$$k_\gamma = P_{ICO_2} - m_\alpha \times P_{IO_2} \quad \text{(A11)}$$

and the slope m_γ is equal to that of the RER line = $+\infty$ in air:

$$m_\gamma = \frac{F_{ICO_2} - 1}{F_{IO_2}} \quad \text{(A12)}$$

On this basis, starting from Equation A1, we know that the exponential plateau *c* corresponds to the straight line γ; therefore:

$$c = \frac{P_{ACO_2} - P_{ICO_2} + m_\alpha \times P_{IO_2}}{m_\gamma} \quad \text{(A13)}$$

Equations A1 and A7 are tangent in point B, thus their first derivative at this point must be equal. This allows a definition of determinant *b* of Equation A1 as:

$$b = \frac{1}{a \times e^{a \times \text{ss}P_{ACO_2}}} \times \left(\frac{1}{m_\beta} - \frac{1}{m_\gamma}\right) \quad \text{(A14)}$$

Substituting the determinants *c* and *b* in Equation A1 and forcing the curve to pass through point B, we can define the determinant *a*:

$$a = \frac{m_\gamma - m_\beta}{m_\beta \times \left[\left(\frac{m_\gamma}{m_\alpha} - 1\right) \times \left(\text{ss}P_{ACO_2} - P_{ICO_2} + m_\alpha \times P_{IO_2}\right)\right]} \quad \text{(A15)}$$

To sum up, the necessary data for the construction of the extreme hypoventilation loop in BH are as follows: (i) P_B; (ii) the inspired gas composition (P_{IO_2} and P_{ICO_2}); (iii) ssRER; (iv) apnRER; and (v) $\text{ss}P_{ACO_2}$.

In pure oxygen, the pressure balance of alveolar gas transfer across the alveolar–capillary gas barrier is ensured by O_2, meaning that the relationship between P_{AO_2} and P_{ACO_2} becomes:

$$P_{ACO_2} = -P_{AO_2} + P_{IO_2} \quad \text{(A16)}$$

Consequently, lines α, β and γ also coincide with Equation A16, and Equation A1 cannot be applied. The alveolar extreme hypoventilation loop in pure oxygen is reduced to a straight line, starting from the alveolar gas composition that precedes BH and virtually ending at the alveolar gas composition where all the oxygen is replaced by CO_2, i.e. the *y*-intercept of Equation A16.

Given this mathematical model, it is possible to predict the alveolar pathway when BHs are performed while breathing a normobaric hyperoxic gas mixture. In fact, when F_{IO_2} increases progressively above that of ambient air (F_{IO_2} = 0.2093), the necessary straight lines (Figure 1, straight lines α, β and γ) to construct the extreme hypoventilation curve (Figure 1, continuous curve), starting from their positions in ambient air, progressively approach the line describing Equation A16, to coincide with it when $F_{IO_2} = 1$. In fact, the slope of the straight lines α, β and γ (Figure 1 and Equations A3, A9 and A12, respectively) depend on the inspired gas mixture. The lower the nitrogen partial pressure, the closer their slope is to −1 (Rahn & Fenn, 1955). Consequently, when F_{IO_2} is increased above that of inspired air, the alveolar gas pathway becomes flatter (less concave) the higher the F_{IO_2}, to become a straight line coinciding with Equation A16 when $F_{IO_2} = 1$.